The following Communications have been judged by at least two referees to be "very important papers" and will be published online at www.angewandte.org soon:

*A. Staubitz, A. Presa, I. Manners**
Iridium-Catalyzed Dehydrocoupling of Primary Amine–Borane Adducts: A Route to High Molecular Weight Polyaminoboranes, Boron–Nitrogen Analogues of Polyolefins

S. Gerlich, M. Gring, H. Ulbricht, K. Hornberger, J. Tüxen, M. Mayor,* M. Arndt**
Matter-Wave Metrology as a Complementary Tool for Mass Spectrometry

V. L. Blair, L. M. Carrella, W. Clegg, B. Conway, R. W. Harrington, L. M. Hogg, J. Klett, R. E. Mulvey, E. Rentschler, L. Russo*
Tuning the Basicity of Synergic Bimetallic Reagents: Switching the Regioselectivity of Direct Dimetalation of Toluene from 2,5- to 3,5-Positions

*J.-J. Li, T.-S. Mei, J.-Q. Yu**
Synthesis of Indolines and Tetrahydroisoquinolines from Arylethylamines by Palladium(II)-Catalyzed C–H Activation Reactions

*S. G. Srivatsan, N. J. Greco, Y. Tor**
Highly Emissive Fluorescent Nucleoside Signals the Activity of Toxic Ribosome-Inactivating Proteins

M. Mascal, E. B. Nikitin*
Direct, High-Yield Conversion of Cellulose into Biofuel

P. García-Álvarez, D. V. Graham, E. Hevia, A. R. Kennedy, J. Klett, R. E. Mulvey, C. T. O Hara, S. Weatherstone*
Unmasking Representative Structures of TMP-Active Hauser and Turbo Hauser Bases

Books

Highlights

Antibiotics

Following a golden compass: Inhibition of the biosynthesis of staphyloxanthin, a product of the *Staphylococcus aureus* sterol pathway, attenuates the virulence of this bacterial pathogen in mice (see picture of an inhibitor in the active site of the dehydrosqualene synthase of *S. aureus*; C green, O red, S yellow, P orange. Does this proof of principle presage a new class of narrow-spectrum antibiotics that target virulence-specific enzymes?

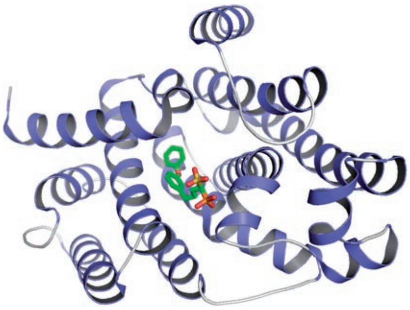

Dual Catalysis

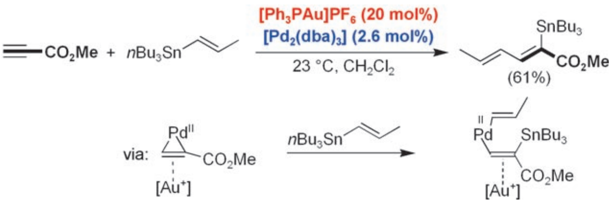

Strong together: Both a gold complex and a palladium complex are needed as catalysts in a Stille-type reaction that does not require an organic halide for the oxidative-addition step (see scheme; dba = *trans*, *trans*-dibenzylideneacetone). The bimetallic catalyst system facilitates the construction of highly substituted olefins. Additional examples of reactions that employ the combined action of a π acid and a cocatalyst are briefly discussed.

Contents

Minireviews

Achiral Chiroptics

K. Claborn, C. Isborn, W. Kaminsky,*
B. Kahr* ______________ **5706 – 5717**

Optical Rotation of Achiral Compounds

Enantiomorphism is not compulsory: Some achiral molecules and crystals can rotate the plane of polarized light when suitably oriented with respect to the wave vector of light. This phenomenon is well known in crystallography, but chemists still take enantiomorphism as a necessary condition for optical rotation or circular dichroism. This Minireview gives an overview of polarimetric measurements of achiral crystals, as well as quantum mechanical computations of the optical activity of simple achiral compounds such as H_2O in the gas phase.

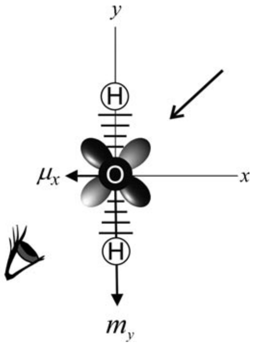

Reviews

Drug Discovery

K. Sakurada,* F. M. McDonald,*
F. Shimada* ______________ **5718 – 5738**

Regenerative Medicine and Stem Cell Based Drug Discovery

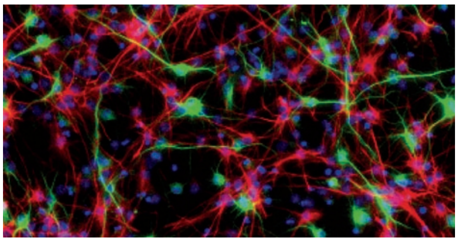

Solving the age-old problem: In our aging society, chronic degenerative diseases are an increasing burden on healthcare systems. The discovery of adult stem cells in many organs of the human body has opened up new possibilities for regenerating failing systems. The picture shows adult stem cells from the brain (cell nuclei: blue, cell bodies: unstained) which can give rise to new neurons (green cells) and astrocytes (red cells), two important cell types in the brain.

Communications

Spin Ladders

H. Kageyama,* T. Watanabe, Y. Tsujimoto, A. Kitada, Y. Sumida, K. Kanamori, K. Yoshimura, N. Hayashi, S. Muranaka, M. Takano, M. Ceretti, W. Paulus, C. Ritter, G. André ______________ **5740 – 5745**

Spin-Ladder Iron Oxide: $Sr_3Fe_2O_5$

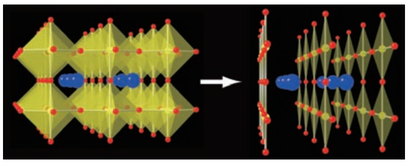

Reduction with CaH_2 of double-layered perovskite $Sr_3Fe_2O_7$ yielded novel two-legged $S=2$ ladder compound $Sr_3Fe_2O_5$. Together with the synthesis of $SrFeO_2$, this opens up new avenues for solid-state chemistry and physics of a series of n-legged ladders $Sr_{n+1}Fe_nO_{2n+1}$. The picture illustrates the structural transformation from FeO_6 octahedra in $Sr_3Fe_2O_7$ to FeO_4 squares in $Sr_3Fe_2O_5$, which occurs via intermediate $Sr_3Fe_2O_6$ (Sr blue, O red, Fe yellow).

For the USA and Canada: ANGEWANDTE CHEMIE International Edition (ISSN 1433-7851) is published weekly by Wiley-VCH, PO Box 191161, 69451 Weinheim, Germany. Air freight and mailing in the USA by Publications Expediting Inc., 200 Meacham Ave., Elmont, NY 11003. Periodicals postage paid at Jamaica, NY 11431. US POSTMASTER: send address changes to *Angewandte Chemie*, Wiley-VCH, 111 River Street, Hoboken, NJ 07030. Annual subscription price for institutions: US$ 7225/6568 (valid for print and electronic / print or electronic delivery); for individuals who are personal members of a national chemical society prices are available on request. Postage and handling charges included. All prices are subject to local VAT/sales tax.

Hybrid Gels

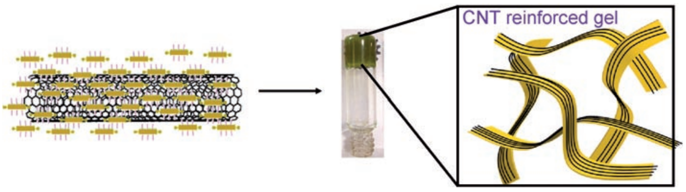

Gel self-assembly: Addition of small amounts of carbon nanotubes (CNTs) to a solution of oligo(*p*-phenylene vinylene) **OPV1** in toluene triggers their self-assembly to form a composite gel (see picture) with higher stability and better rheological properties than the **OPV1** gel. Strong physical interactions between the species allow the encapsulation of CNTs into self-assembled tapes of **OPV1**, reinforcing the 3D gel network.

Bioinspired Materials

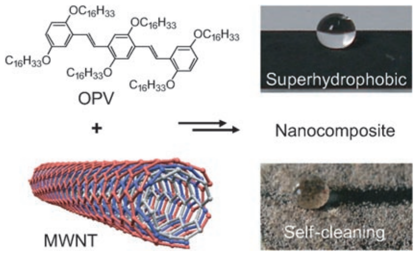

Rough and clean: The physical interaction and self-assembly of oligo(*p*-phenylenevinylene)s (OPVs) on carbon nanotubes (CNTs) allow the dispersion of the latter in organic solvents. This well-dispersed nanocomposite can be coated on to glass, metal, and mica surfaces to give superhydrophobic self-cleaning surfaces with water contact angles of 165–170° and a sliding angle of less than 2° (see picture).

Ion Channels

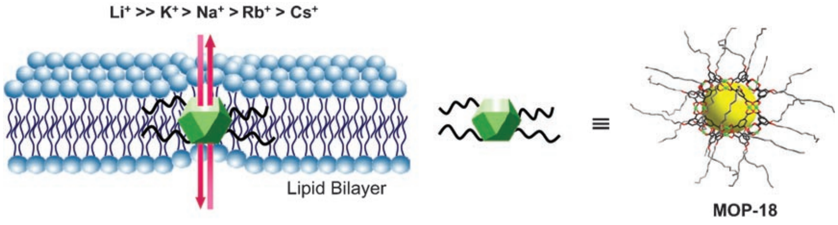

MOPping up ions: A synthetic ion channel formed with MOP-18 transports protons and alkali-metal ions across lipid membranes. Homogeneous, long-lived single-channel currents were observed in planar lipid bilayer experiments. The MOP-18 channel prefers cations over anions, and the cation selectivity is in the order $Li^+ \gg Na^+ > K^+ > Rb^+ > Cs^+$. This system is promising for applications such as sensors and catalysis.

Alkene Hydrochlorination

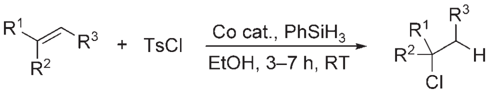

A simple solution to a long-standing problem: The hydrochlorination of unactivated alkenes, which is shown in the Scheme, is catalyzed by simple cobalt complexes and proceeds under very mild conditions. The ready availability of all components and the ease of execution render the method very convenient.

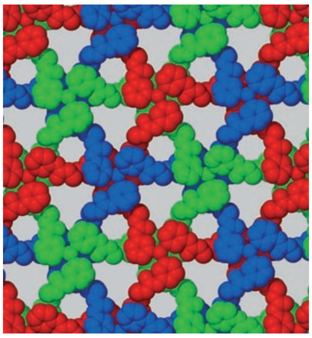

Weave done it! The reaction of ligands with binding sites for anions and metal ions with silver nitrate has led to the formation of a series of Borromean weave coordination polymers (each network is color coded in the picture). These possess anion-binding and neutral guest inclusion compartments that are occupied by various solvent molecules.

Coordination Networks

P. Byrne, G. O. Lloyd, N. Clarke, J. W. Steed* ______ **5761 – 5764**

A "Compartmental" Borromean Weave Coordination Polymer Exhibiting Saturated Hydrogen Bonding to Anions and Water Cluster Inclusion

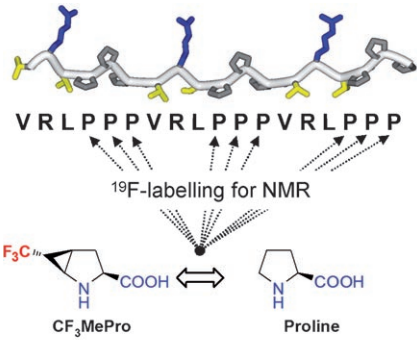

As good as a Pro: Another CF_3-substituted amino acid, CF_3MePro (see structure), has been added to the arsenal of ^{19}F NMR labels; it is particularly suited for the study of proline-rich peptides. This amino acid was carefully designed and chosen from other synthesized isomers, according to strict selection criteria, as the most stable, nonracemizable, conformationally restricted, and compatible with solid-phase peptide-synthesis protocols.

Amino Acids

P. K. Mykhailiuk, S. Afonin, G. V. Palamarchuk, O. V. Shishkin, A. S. Ulrich,* I. V. Komarov* **5765 – 5767**

Synthesis of Trifluoromethyl-Substituted Proline Analogues as ^{19}F NMR Labels for Peptides in the Polyproline II Conformation

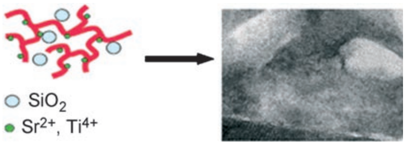

Film formation: Polymer-assisted deposition allows the growth of nanocomposite thin films comprising amorphous silica nanoparticles embedded in epitaxial $SrTiO_3$ and $CoFe_2O_4$ matrices (see picture). These silica nanoparticles can be as small as 10 nm and become larger with increasing post annealing temperature. The incorporation of silica into epitaxial $CoFe_2O_4$ films greatly enhances its coercivity and magnetic anisotropy.

Nanocomposites

H. M. Luo,* Y. Lin, H. Wang, S. A. Baily, J. H. Lee, M. E. Hawley, T. M. McCleskey, A. K. Burrell, E. Bauer, L. Civale, Q. X. Jia* ______ **5768 – 5771**

Amorphous Silica Nanoparticles Embedded in Epitaxial $SrTiO_3$ and $CoFe_2O_4$ Matrices

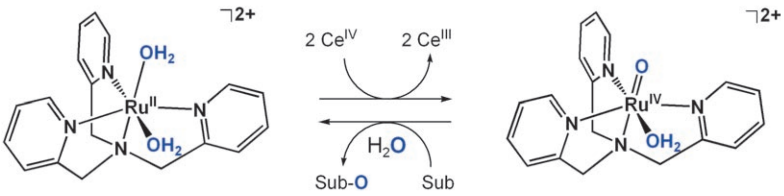

Water is not only the solvent but also the sole oxygen source in the smooth and efficient oxidation of organic compounds catalyzed by a Ru^{II}–pyridylamine–aqua complex with Ce^{IV} as the oxidant. An intermediate-spin Ru^{IV}–oxo complex is formed as the reactive species (see scheme; Sub = substrate). This catalytic system is durable and able to gain high turnover numbers for various substrates.

Oxygenation in Water

Y. Hirai, T. Kojima,* Y. Mizutani, Y. Shiota, K. Yoshizawa, S. Fukuzumi* **5772 – 5776**

Ruthenium-Catalyzed Selective and Efficient Oxygenation of Hydrocarbons with Water as an Oxygen Source

Metal–Organic Frameworks

C. Scherb, A. Schödel,
T. Bein* 5777 – 5779

Directing the Structure of Metal–Organic Frameworks by Oriented Surface Growth on an Organic Monolayer

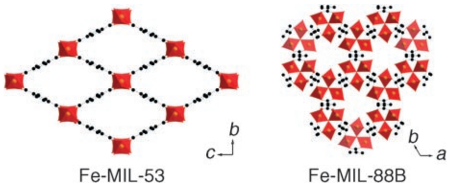

Orientation and structure of porous metal–organic frameworks (MOFs) based on iron and 1,4-benzenedicarboxylic acid can be controlled by heterogeneous nucleation on self-assembled monolayers of mercaptohexadecanoic acid (MHDA). Thus, the product of homogeneous nucleation is the MOF Fe-MIL-53, whereas in the same crystallization solution, oriented Fe-MIL-88B grows on a MHDA-functionalized gold surface (see picture).

Host-Guest Chemistry

K. Suzuki, J. Iida, S. Sato, M. Kawano,
M. Fujita* 5780 – 5782

Discrete and Well-Defined Hydrophobic Phases Confined in Self-Assembled Spherical Complexes

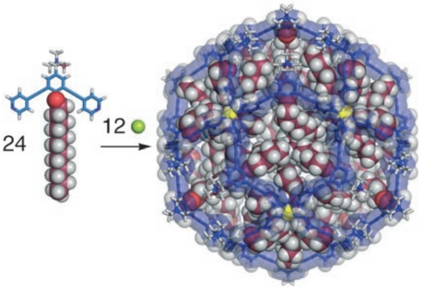

Interior design: A 5 nm sized spherical complex, which confines 24 alkyl chains in its interior, provides a localized hydrophobic environment with a uniform size and structure (see picture; shell blue, Pd yellow, O red, C purple, H gray). The hydrophobic phase can solubilize dye molecules, and the hydrophobicity of the complex can be tuned by simply changing the length of the alkyl chains.

C–H Activation

J. Zhou, J. F. Hartwig* 5783 – 5787

Iridium-Catalyzed H/D Exchange at Vinyl Groups without Olefin Isomerization

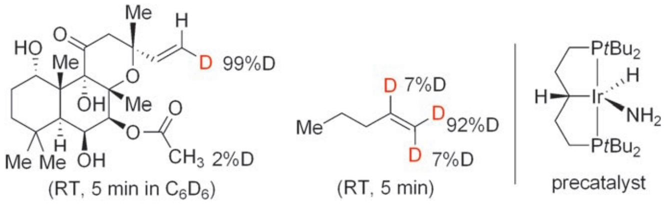

Making the switch: The title reaction represents a rare example of olefinic C–H activation without olefin isomerization. The conditions are sufficiently mild so that functional groups such as ketones, esters, nitriles, amines, sulfides, and alcohols are tolerated. This selectivity is demonstrated by deuterium labeling of several complex molecules.

Natural Products Synthesis

J.-J. Shie, J.-M. Fang,*
C.-H. Wong 5788 – 5791

A Concise and Flexible Synthesis of the Potent Anti-Influenza Agents Tamiflu and Tamiphosphor

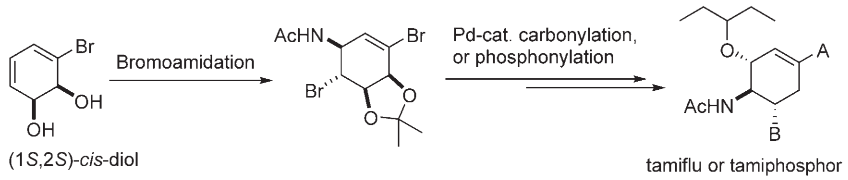

Tamiflu and the highly potent neuraminidase inhibitor tamiphosphor have been synthesized in 11 steps and greater than 20% overall yields from an haloarene (1*S*,2*S*)-*cis*-diol. The key transformations include a regio- and stereoselective bromoamidation, and a palladium-catalyzed carbonylation or phosphonylation reaction (see scheme; tamiflu: A = CO_2Et, B = $NH_3^+H_2PO_4^-$, tamiphosphor: A = $PO(ONH_4)_2$, B = NH_2).

Copper complexes with a CO$_2$ fixation: Copper(I) complexes serve as excellent catalysts for the carboxylation of aryl- and alkenylboronic esters with CO$_2$, affording a variety of functionalized carboxylic acid derivatives (see scheme). Important active intermediates such as the copper(I) aryl and carboxylate complexes, [(IPr)CuR] and [(IPr)CuOCOR] (R = 4-MeOC$_6$H$_4$, IPr = 1,3-bis(2,6-diisopropylphenyl)imidazol-2-ylidene), are isolated and structurally characterized.

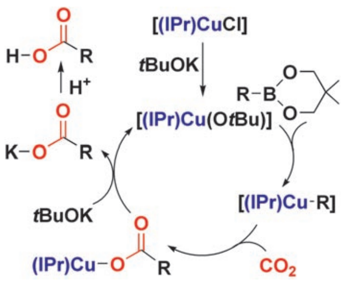

Homogeneous Catalysis

T. Ohishi, M. Nishiura, Z. Hou* **5792 – 5795**

Carboxylation of Organoboronic Esters Catalyzed by N-Heterocyclic Carbene Copper(I) Complexes

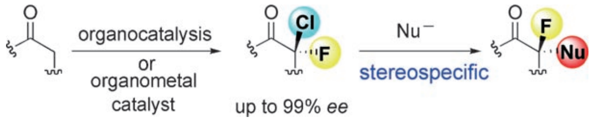

"F-antastic" chiral molecules: Asymmetric syntheses of α,α-chlorofluoro carbonyl compounds have been developed. Nucleophilic substitutions of an α,α-chlorofluoroketone thus obtained with azide or thiol nucleophiles provide various optically active fluorinated compounds without loss of optical purity (see scheme).

Fluorinated Molecules

K. Shibatomi,* H. Yamamoto* **5796 – 5798**

Stereoselective Synthesis of α,α-Chlorofluoro Carbonyl Compounds Leading to the Construction of Fluorinated Chiral Quaternary Carbon Centers

A W≡Pb bond is present in the hydrido plumbylidyne complex *trans*-[H(PMe$_3$)$_4$W≡Pb(2,6-Trip$_2$C$_6$H$_3$)], which is formed by an unprecedented Pb–N activation reaction of {Pb(2,6-Trip$_2$C$_6$H$_3$)NMe$_2$}$_2$, the first structurally characterized organolead(II) amide (see picture for molecular structure). Trip = 2,4,6-*i*Pr$_3$C$_6$H$_2$.

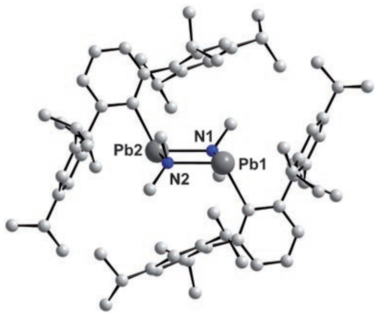

Plumbylidyne Complexes

A. C. Filippou,* N. Weidemann, G. Schnakenburg **5799 – 5802**

Tungsten-Mediated Activation of a Pb^{II}–N bond: A New Route to Tungsten–Lead Triple Bonds

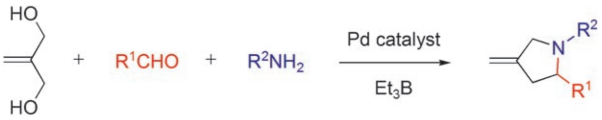

A straightforward route: The combination of a palladium catalyst and triethylborane promotes the amphiphilic (nucleophilic–electrophilic) allylation of aldimines, prepared in situ from a wide variety of aromatic and aliphatic aldehydes and amines, with commercially available 2-methylenepropane-1,3-diols to provide pyrrolidines (see scheme).

Amphiphilic Allylation

M. Kimura,* T. Tamaki, M. Nakata, K. Tohyama, Y. Tamaru* **5803 – 5805**

Convenient Synthesis of Pyrrolidines by Amphiphilic Allylation of Imines with 2-Methylenepropane-1,3-diols

Contents

Silica Nanostructures

T. Zhang, J. Ge, Y. Hu, Q. Zhang, S. Aloni, Y. Yin* ______ 5806–5811

Formation of Hollow Silica Colloids through a Spontaneous Dissolution–Regrowth Process

From the inside out: Silica colloids can be spontaneously transformed from solid spheres to hollow structures in aqueous solutions of NaBH$_4$ (see picture). The high pH value and gradual decomposition of NaBH$_4$ facilitate the formation of hollow structures first by partial dissolution of silica cores and then by regrowth of the silicate species on the colloid surfaces to form shells.

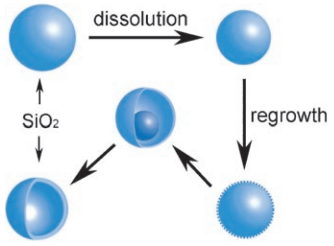

Organocopper Reagents

R. Bomparola, R. P. Davies,* S. Hornauer, A. J. P. White ______ 5812–5815

Structural Characterization of Magnesium Organocuprates Derived from Grignard Reagents: Cu$^{\text{I}}$-Based Inverse Crown Ethers

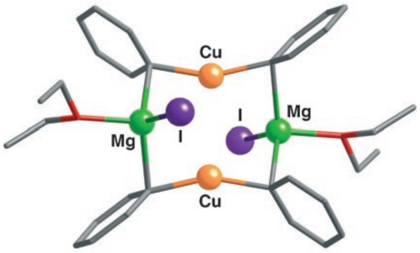

Shared interests: The structures of the title compounds (see example) were found to be directly comparable to those of lithium organocuprates, with the formal replacement of the lithium cation with a magnesium halide cation. Furthermore, both types of organocuprates form contact ion pairs in weakly coordinating solvents and solvent-separated ion pairs in strongly coordinating solvents.

Catalyst Design

K. Albahily, E. Koç, D. Al-Baldawi, D. Savard, S. Gambarotta,* T. J. Burchell, R. Duchateau* ______ 5816–5819

Chromium Catalysts Supported by a Nonspectator NPN Ligand: Isolation of Single-Component Chromium Polymerization Catalysts

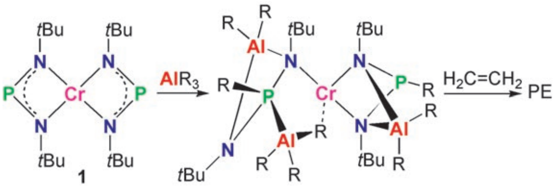

Switchable catalytic activity, from nonselective ethylene oligomerization to trimerization and even polymerization, is shown by **1**, depending on the alkyl aluminum compound with which it is activated. AlMe$_3$ or *i*Bu$_2$AlCl resulted in highly active single-component polymerization catalysts (see scheme; R = Me, PE = polyethylene), the activity of which can be switched or inhibited by the presence of an additional alkyl aluminum compound.

Synthetic Methods

D. Hojo, K. Noguchi, M. Hirano, K. Tanaka* ______ 5820–5822

Enantioselective Synthesis of Spirocyclic Benzopyranones by Rhodium-Catalyzed Intermolecular [4+2] Annulation

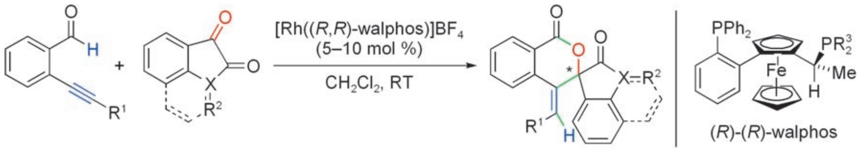

Rounding things off: A cationic Rh$^{\text{I}}$/(*R*,*R*)-walphos complex catalyzes an enantioselective [4+2] annulation of 2-alkynylbenzaldehydes with cyclic electron-deficient carbonyl compounds at room temperature (see scheme, R^3 = 3,5-(F$_3$C)$_2$C$_6$H$_3$, X = C or N). Enantioenriched spirocyclic benzopyranones and isatin derivatives are obtained in high yield (up to 97 %) and high enantioselectivity (up to > 99 %).

Structure Elucidation

Y. L. Zhang, H. M. Ge, W. Zhao, H. Dong, Q. Xu, S. H. Li, J. Li, J. Zhang, Y. C. Song, R. X. Tan* ———— 5823 – 5826

Unprecedented Immunosuppressive Polyketides from *Daldinia eschscholzii*, a Mantis-Associated Fungus

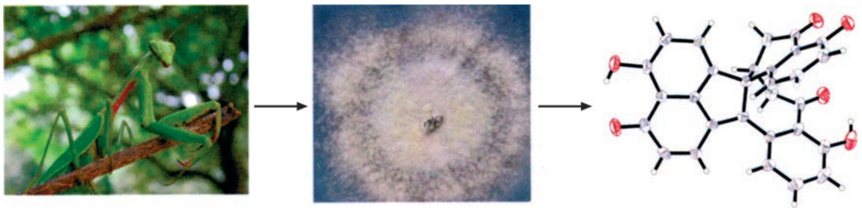

Going with a gut reaction: Dalesconols A (structure shown) and B were discovered in the title fungus (middle picture) derived from the mantis gut. The novel architecture and biological profiles of these natural products make the dalesconols attractive lead compounds for the development of immunosuppressive agents.

Natural Products

K. Liu, A. Chougnet, W.-D. Woggon* ———— 5827 – 5829

A Short Route to α-Tocopherol

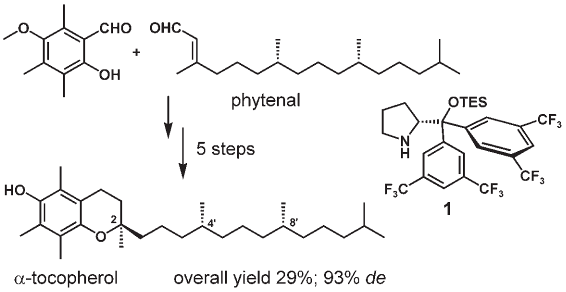

Short and sweet: A simple and practical route to α-tocopherol is described (see scheme; TES = triethylsilyl). The key step is a remarkably diastereoselective domino aldol/oxa-Michael reaction, which is promoted by proline derivative **1**.

Water Oxidation

J. Mola, E. Mas-Marza, X. Sala, I. Romero,* M. Rodríguez, C. Viñas, T. Parella, A. Llobet* ———— 5830 – 5832

Ru-Hbpp-Based Water-Oxidation Catalysts Anchored on Conducting Solid Supports

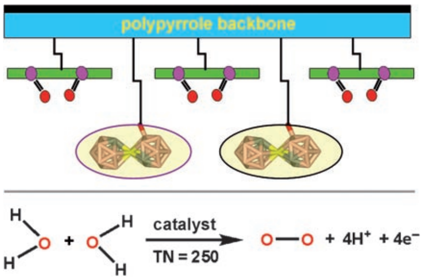

Splitting water: Copolymerization of the cationic water-oxidation catalyst $[Ru_2^{II}(\mu\text{-bpp})(t\text{-trpy})_2(H_2O)_2]^{3+}$ (**1**) with a cobalt cobaltabisdicarbollide monomer (**2**) generates a new material, "FTO/poly-(**1**-*co*-**2**)", that is capable of oxidizing water to molecular dioxygen with a turnover number (TN) of 250 (see picture). This represents the best performance ever obtained in a heterogeneous phase using a chemical oxidant.

Organosilver Reagents

K. Murakami, K. Hirano, H. Yorimitsu,* K. Oshima* ———— 5833 – 5835

Silver-Catalyzed Transmetalation between Chlorosilanes and Aryl and Alkenyl Grignard Reagents for the Synthesis of Tetraorganosilanes

$$R_3Si{-}Cl + ArMgBr \xrightarrow[\text{THF, 25 °C or below}]{\text{cat. AgNO}_3} R_3Si{-}Ar$$

The silver savior: Nucleophilic substitution reactions of chlorosilanes with aryl Grignard reagents have been developed which take place under silver catalysis to afford tetraorganosilanes (see scheme). This transformation is likely to be promoted by diarylargentate reagents that are generated in situ.

Asymmetric Catalysis

M. Rueping,*
A. P. Antonchick ______ **5836 – 5838**

A Highly Enantioselective Brønsted Acid Catalyzed Reaction Cascade

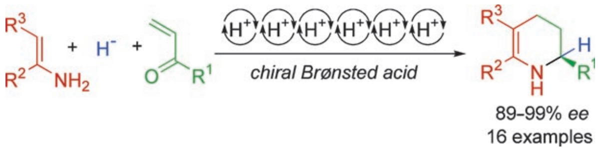

One cat. is enough! A highly enantioselective reaction has been developed for the three-component reaction of an enamine with a vinyl ketone and a Hantszsch ester in which each of the six reaction steps is catalyzed by the same chiral Brønsted acid (see scheme). This reaction offers efficient access to tetrahydropyridines and azadecalinones from simple and readily available starting materials.

Amyloids

C. Wasmer, A. Soragni, R. Sabaté,
A. Lange, R. Riek,
B. H. Meier* ______ **5839 – 5841**

Infectious and Noninfectious Amyloids of the HET-s(218–289) Prion Have Different NMR Spectra

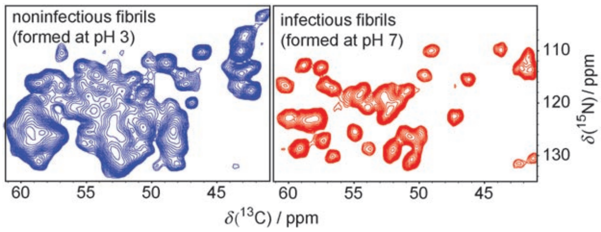

The molecular basis for prion infectivity is not yet understood. The NMR spectra of noninfectious and infectious amyloids of the prion-forming domain 218–289 of the fungal prion HET-s are clearly different (see picture) but are indicative for a cross-β arrangement in both cases. The fibrils formed at pH 3 are not infectious because their molecular structure apparently differs substantially from that formed at physiological pH.

Fibril Formation

R. Verel, I. T. Tomka, C. Bertozzi,
R. Cadalbert, R. A. Kammerer,
M. O. Steinmetz,
B. H. Meier* ______ **5842 – 5845**

Polymorphism in an Amyloid-Like Fibril-Forming Model Peptide

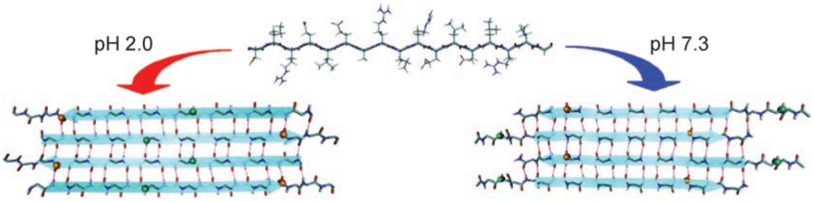

The structural basis for polymorphism in amyloids is unraveled with a model system. The hydrogen-bonding pattern within the β sheets of fibrils is strongly influenced by the pH of the solution from which the fibrils are formed. Solid-state NMR spectroscopy experiments allow quantification of the relative amounts of two different β-sheet structures over the pH range 2.0–7.3.

Solid Solutions

M. Schmidt, T. Stumpf,*
M. Marques Fernandes, C. Walther,
T. Fanghänel ______ **5846 – 5850**

Charge Compensation in Solid Solutions

Compensating differences: The formation of solid solutions is still not fully understood. A basic principle requiring clarification is the charge compensation mechanism upon incorporation of differently charged ions. Spectroscopic measurements show how coupled substitution of Na^+ with Eu^{3+}/Cm^{3+} can provide charge compensation when incorporating trivalent lanthanides into calcite on the Ca^{2+} site.

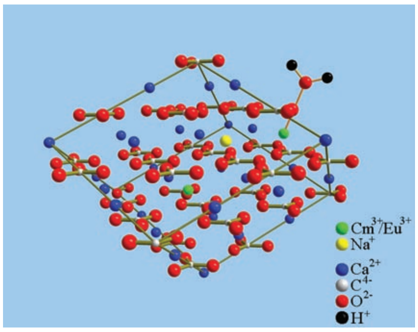

NMR Spectroscopy

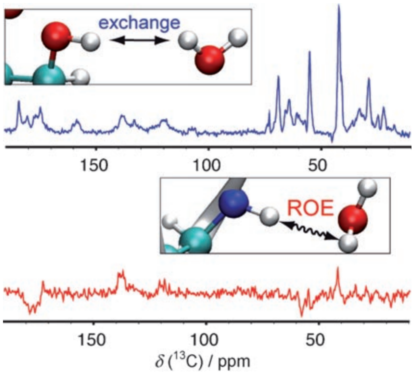

A key to the elucidation of protein functions are water–protein interactions. The determination of polarization-transfer pathways between water and immobilized proteins demonstrates that chemical exchange (sometimes followed by spin diffusion) is the dominant mechanism. At low temperatures or high spinning frequencies, this pathway becomes inefficient, and intermolecular NOEs are observed (see NMR spectra; ROE = rotating frame NOE).

Supporting information is available on www.angewandte.org (see article for access details).

A video clip is available as Supporting Information on www.angewandte.org (see article for access details).

Service

www.chemasianj.org

www.chemmedchem.org

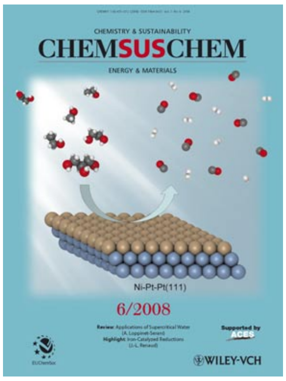

www.chemsuschem.org